Bioprocess and Biosystems Engineering
https://doi.org/10.1007/s00449-020-02446-x

RESEARCH PAPER

Enhancing electrochemical sensing for catechol by biomimetic oxidase covalently functionalized graphene oxide

Xia Jiaojiao[1] · Wang Pengyun[1] · Zou Bin[1] · Adesanya Idowu Onyinye[1]

Received: 18 May 2020 / Accepted: 9 September 2020

Abstract

Catechol level is an important indicator for evaluating the quality of tea. Therefore, the exploration of a simple and efficient quantitative detection method for catechol has an important significance. In this study, functionalized graphene oxide was synthesized by chemically modifying the surface of graphene oxide. The prepared carrier was covalently combined with biomimetic oxidase iron porphyrin (FePP, the active center of horseradish peroxidase). Ionic liquid as covalent coupling agents was designed as electronic bridge between biomimetic oxidase and graphene oxide. The novel biomimetic biosensor provided a detection range of 50.0–1600.0 μmol/L by modulating under the optimal conditions of the reaction system (FePP concentration is 1.5×10^{-3} mol/L, pH 3.0, Nafion solution dosage 1% and temperature 25 °C), the detection limit is 0.09 μmol/L. The biosensor has excellent stability, repeatability and reproducibility, and is expected to be applied to the rapid detection of catechol in actual tea sample..

Graphic abstract

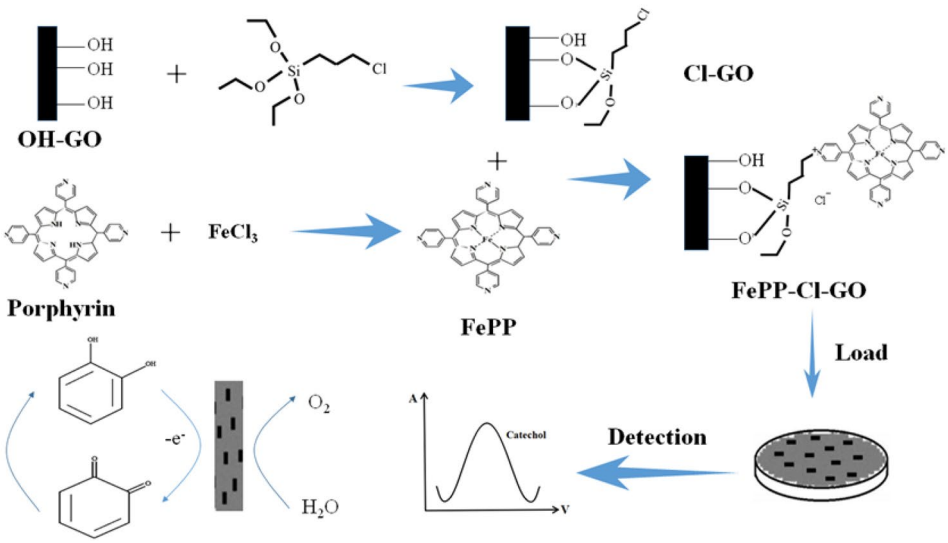

Keywords Biomimetic oxidase · Iron porphyrin · Graphene oxide · Functionalized surface · Catechol

Introduction

In light of anti-oxidation, anti-virus, prevention of the accumulation of harmful proteins and protection of brain cells, catechol, a natural component of tea has attracted much

✉ Zou Bin
binzou2009@ujs.edu.cn

[1] School of Food and Biological Engineering, Jiangsu University, No.301 Xuefu Road, Zhenjiang 212013, China

Published online: 23 September 2020

attention recently. It has become one of the important indicators for judging tea quality [1]. Developing a simple and efficient quantitative detection method for catechol is thus of important significance for the evaluation of comprehensive quality of tea and human health.

Extensive methods have been used in recent years to detect catechol, including spectrophotometry, flow injection and high-performance liquid chromatography [2]. These different techniques are reliable, but their cumbersome and costly operation, time-detection is a major technical problem hindering their large-scale application. Therefore, a fast and convenient method is desirable for practical application. Nowadays, efficient electrochemical biosensor technology is a potential alternative to the detection of catechol [3–5]. Albayati et al. [6] introduced a novel electrode for catechol detection by covalent immobilization of laccase (Lac) on a glassy carbon electrode modified by gold nanoparticles (AuNPs) and carboxylated multiwalled carbon nanotubes(c-MWCNTs). The catechol detection limit was 12.26 μM. Similar low detection limit of 3.75 μM was also reported using active center iron porphyrin (FePP) of the horseradish peroxidase (HRP) instead of above laccase in our previous study [7]. Although FePP sensor was economical and sensitive, FePP was non-covalently immobilized on different functionalized carbon nanotubes for the detection of catechol. The stability was far below the actual application requirement due to simple physical adsorption. The exploration of more stable sensors and sensing materials were critical for catechol detection.

Graphene was almost the best sensing material and far beyond other material, including electron mobility of 2×10^5 $cm^2/V{\cdot}s$ (about 140 times of silicon), sheet resistance of only 30 Ω/m and specific surface area of 3000 m^2/g [8]. However, graphene was chemically inert and its atomically smooth surface hindered the adherence of active substances. Activation of graphene to form graphene oxide (GO) and further covalently fix active substances by molecule coupling to improve the stability of the sensor has been attempted [9]. Qi Yunlong et al. [10] induced stable cross-linked graphene oxide hydrogel using Co^{2+} and pyrrole, followed by doping nitrogen and sulfur atoms into graphene sheets to obtain 3D N-S-doped graphene electrodes. The detection limit for catechol detection was 0.15 μM. Seyma Erogul et al. [11] prepared a novel sensor based on Fe_3O_4 functionalized graphene oxide and gold nanoparticle composite to detect catechol. The detection limit was 0.8 μM under optimized conditions.

In this study, an original combination of biomimetic oxidase FePP as biosensor, graphene oxide as sensing material, and ionic liquids as covalent coupling agent was designed and conducted as electrode to detect catechol. Conjugation of the ionic liquid functionalized graphene oxide and the stable FePP rendered the biomimetic oxidase sensor as a candidate for the detection of catechol. Using the ionic liquid modified graphene oxide to covalently immobilize the FePP, it was expected that the stability and electron transfer ability of the biosensor was improved. Nafion polymer solution was used to further enhance the stability of the electrode. Finally, optimal FePP biosensor for catechol detection was obtained by optimizing the reaction conditions, including the concentration of FePP and nafion solution, pH, and temperature. Theoretical basis for the quantitative detection of catechol and rapid evaluation technique of the comprehensive quality of tea were expected to be provided in future.

Experiments

Materials

Graphene oxide gel (1 wt%) and 5, 10, 15, 20-tetra (4-pyridyl) porphyrin were supplied by Aladdin (Shanghai, China). Catechol, potassium ferricyanide, potassium ferrocyanide, ferric/potassium/magnesium/sodium chloride, absolute ethanol, *N*, *N*-dimethylformamide (DMF), theanine, glucose, inorganic salts (NaCl, $(CH_3COO)_2$ $Zn.2H_2O$, $MgSO_4$, KBr), Tris and chloropropyltriethoxysilane were purchased from Sinopharm Group Co. Ltd, China. Perfluorosulfonic acid ion exchange resin [Nafion dispersion, 5% (w/w)] was purchased from Sigma-Aldrich. Green tea was produced by Suzhou Dongshan Tea Factory Co., Ltd and purchased from local supermarket. All the reagents were of analytical grade without further purification. Different pH buffers (0.1 mol/L) were prepared by mixing variable ratios of citric acid and Na_2HPO_4.

Preparation of carrier and iron porphyrin

Preparation of chloropropyl functionalized graphene oxide

5 g of chloropropyltrimethoxysilane was added into 30 mL of absolute ethanol in a round bottom flask. After being uniformly dispersed via ultrasound, 5 g of graphene oxide gel was introduced into the system. The solution was sealed and stirred at room temperature for 24 h. After complete reaction, the obtained solid was isolated by filtration and repeatedly washed with absolute ethanol to give chloropropyl functionalized graphene oxide (Cl–GO for short) (see Fig. 1) [12].

Preparation of iron porphyrin

$FeCl_3$ and 1 g of 5, 10, 15, 20-tetra (4-pyridyl) porphyrin with mole ratio of 2:1 were subjected into a 250 mL round bottom flask. After complete dispersal, 50 mL of DMF was added, and the mixture was further stirred at 160 °C for 12 h

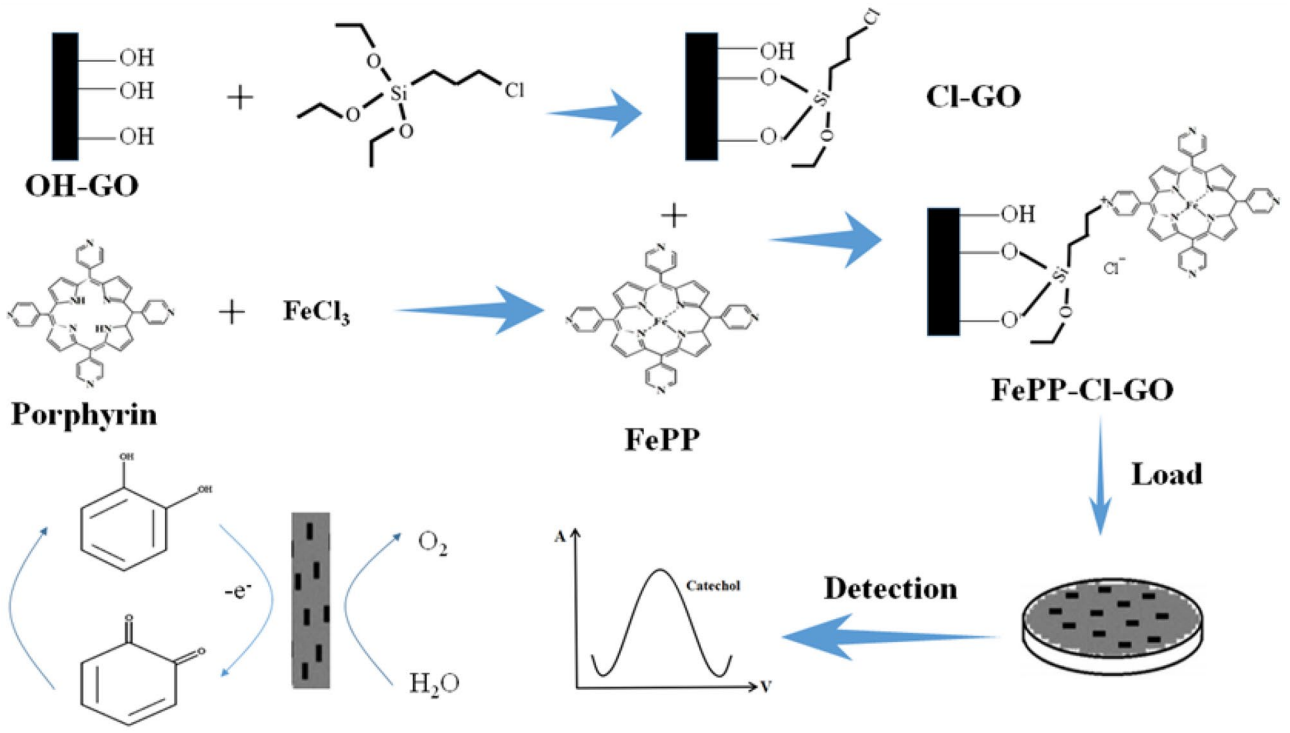

Fig. 1 Illustration of biosensor synthesis and catechol detection

[13]. Afterward, the resulting mixture was cooled to room temperature, filtered, washed with distilled water to remove unreacted salt. The obtained solid was dried at 60 °C for 24 h in a vacuum dryer to remove DMF. The final product was denoted as FePP (see Fig. 1).

Preparation of graphene oxide covalently immobilized FePP biomimetic enzyme

0.5 mmol of iron porphyrin, 1 g of CL–GO, and 50 mL of DMF in a round bottom flask were sonicated for 10 min. After 24 h of reflux condensation, the suspension was cooled to room temperature, filtered, washed with DMF and distilled water 2–3 times, vacuum dried at 60 °C for 24 h to obtain ionic liquid functionalized graphene oxide supported FePP biomimetic enzyme sensor. The composite was denoted as FePP–Cl–GO (see Fig. 1) [9].

Preparation of biosensor electrodes

The electrode was repeatedly polished with 0.10 μm and 0.05 μm alumina and sonicated with distilled water for 15 min until the surface was mirrored. 10 mg of FePP–Cl–GO (or Cl–GO or GO) was weighed and mixed with 1 mL of buffer (pH 7.0). After sonicated for 15 min, carrier dispersion was obtained [14]. Afterward, 10 μL of the carrier dispersion was dropped onto the bare electrode surface and dried with an infrared lamp for 20 min. 1% of Nafion solution prepared via dissolving 10 μL of Nafion dispersion in 1 mL of buffer (pH 7.0) was further instilled into the system and was dried with an infrared lamp for another 20 min. The final dried product FePP–Cl–GO/Nafion/GCE (or Cl–GO/GCE/Nafion/or GO/Nafion/GC) electrode was kept at 4 °C for further use. Similarly, FePP/Nafion/GCE and Nafion/GCE electrodes were synthesized.

Electrochemical detection of catechol

The electrochemical properties of the electrode were characterized by CV and impedance method using 5 mmol/L $[Fe(CN)_6]^{3-/4-}$ solution as substrate. Catechol was detected by biosensors via CV method using different concentrations of pH 3.0 catechol solutions as substrate [7]. Spike recovery rate was calculated to judge the practical application value of the biosensor [15]. Spike recovery rate was obtained by adding a quantitative standard substance to the blank sample matrix, and analyzing the ratio of the actual result to the theoretical value. DPV curves peak current of FePP–Cl–GO/Nafion/GCE electrode were obtained in air-saturated solution with the concentrations of catechol varying from 5.0 to 1600.0 μmol/L in 0.1 mol/L PBS buffer (pH 3.0) at 25 °C. Related parameters in DPV detection: Increment: 0.004 V, amplitude: 0.05 V, pulse width: 0.05 s, sampling width:

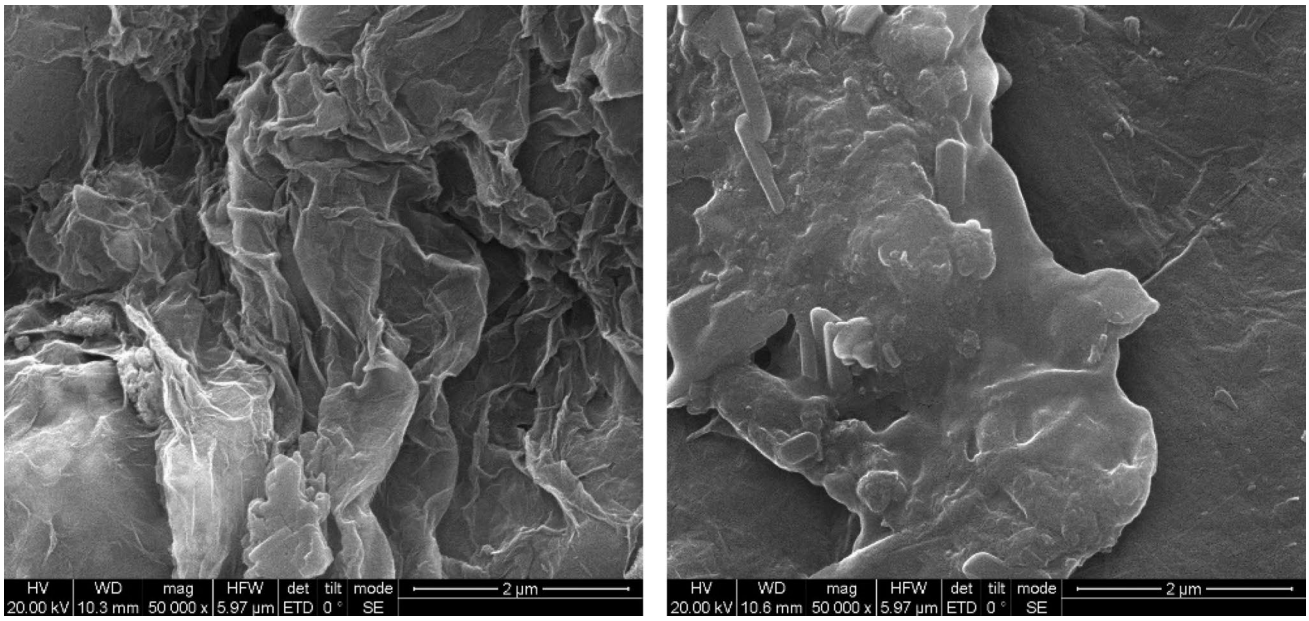

Fig. 2 SEM images of GO (left) and FePP–Cl–GO (right) materials

0.0167, pulse period: 0.5 s. The reference electrode type was Ag/Agcl electrode.

Catechol detection in tea and water samples

1.0 g of tea was weighed, and then crushed in a pulverizer. The powder and 60 mL of 20% methanol were added into a 100 mL beaker. The mixture was heat-treated at 80 °C for 20 min, filtered. The volume of the supernatant was adjusted to 1000 mL with pH 3.0 buffer, and the tea sample was finally obtained. The tea sample was also analyzed by HPLC (Shimadzu Technology, model 20AB). The samples were separated at using a reverse-phase C18 column (200 mm × 4.6 mm). The mobile phase was 20% methanol solution at the flow rate of 0.5 mL·min^{-1}. The catechol concentration in the real tea and water samples was calculated from the calibration curve by the standard addition method.

Characterization

SEM micrographs were collected via JSM-7500F to analyze the surface morphology of FePP–GO and GO with the resolution of 1.4 nm and the pressure of 30 kV. FT-IR spectra of GO, FePP, FePP–GO, and CL–GO were obtained in Nicolet-460 using the standard KBr disk method. The test was conducted in the 4000–400 cm^{-1} with the resolution of 0.4 cm^{-1}. CV and DPV were performed with a chi660D electrochemical workstation (Shanghai Chenhua

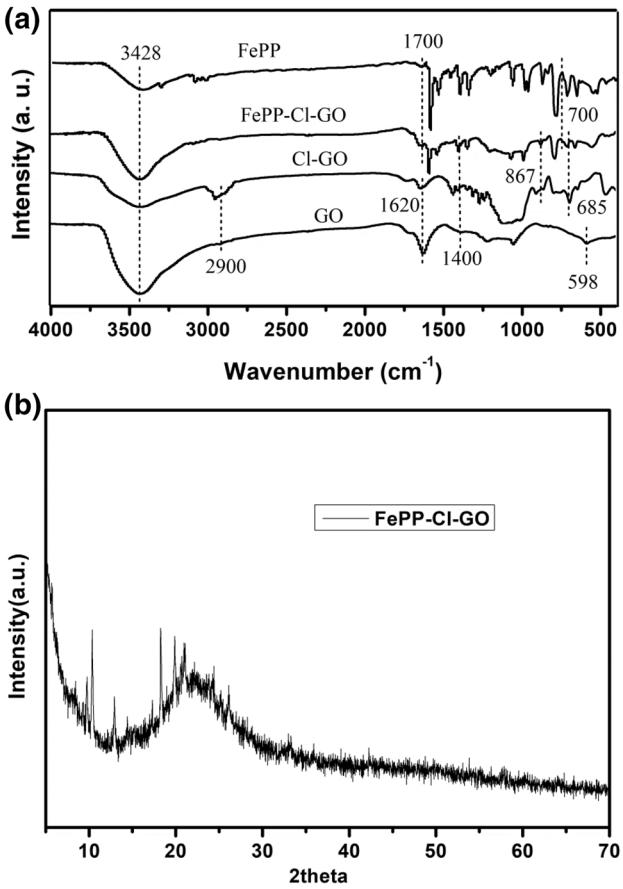

Fig. 3 FT-IR spectrum of GO, Cl–GO, FePP, FePP–GO materials

Co., Ltd. China). All experiments were performed using a three-electrode system (the glassy carbon electrode was the working electrode, the Ag/AgCl electrode was the reference electrode, and the platinum wire electrode was the counter electrode).

Results and discussion

Surface characterization of the modified electrodes

The SEM micrograph of GO shown in Fig. 2 (left) directly noted the fluffy distribution and loose connection between each layer. In sharp contrast, the structure of FePP–Cl–GO shown in Fig. 2 (right) became a multi-layer and compact after covalent immobilization [16]. The functionalized GO mainly served as a bridge to provide an intermediary channel for the surface of the glassy carbon electrode and FePP, and obtained the electron transfer requirement of the electrode surface.

Figure 3a presented the FT-IR spectrum of GO, Cl–GO, FePP, FePP–GO materials. Obvious peaks at 3428, 2900, 1620, 1400, and 598 cm^{-1} corresponding to O–H, C–H stretching, C=O adsorption in the aromatic ring, C=C and O–C stretching were typical bands of GO [17]. For Cl–GO, the skeleton characteristic peaks of GO were observed, and the slightly weakened peak density of O–H was the silicidation of GO due to the introduction of ionic liquid [18]. The presence of peaks at 867 and 685 cm^{-1} were assigned to the stretching vibrations of Si–O–H and Si–O–C [19]. These behaviors indicated that the ionic liquid was successfully grafted onto the surface of GO. The band of FePP–Cl–GO was obviously weaker than that of FePP. Besides, the peak position was shifted compared with CL–GO due to the covalent interaction between FePP and Cl–GO. The N–H and C–H of the pyrrole ring showed typical symmetrical and asymmetrical stretching bands in the range of 700–1700 cm^{-1} [20]. It was indicated that the FePP was successfully immobilized in the GO carrier to form an immobilized FePP biomimetic enzyme. Figure 3b presented the XRD of FePP–GO materials. A diffraction peak of GO was observed at 10.26° corresponding to an interlayer spacing with crystal plane of (001). One more broad diffraction peak was observed at 26.5° crystal plane of

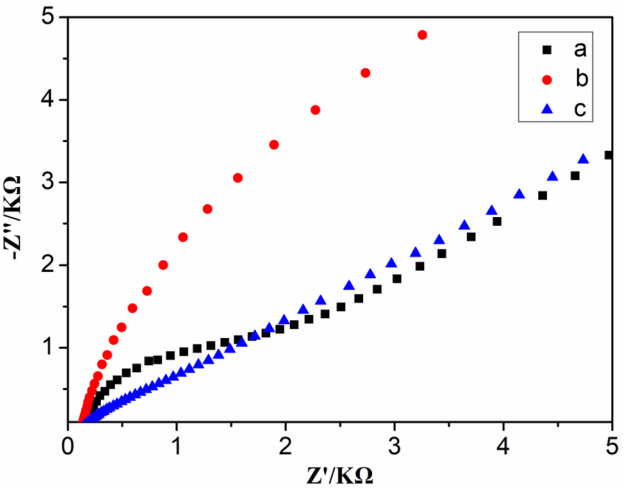

Fig. 5 EIS of **a** Bare GCE, **b** Cl–GO/GCE, **c** FePP–Cl–GO/GCE in the 0.1 mol/L PBS (pH 7.0) containing 5.0 mmol/L $[Fe(CN)_6]^{3-/4-}$ and 0.1 mol/L KCl

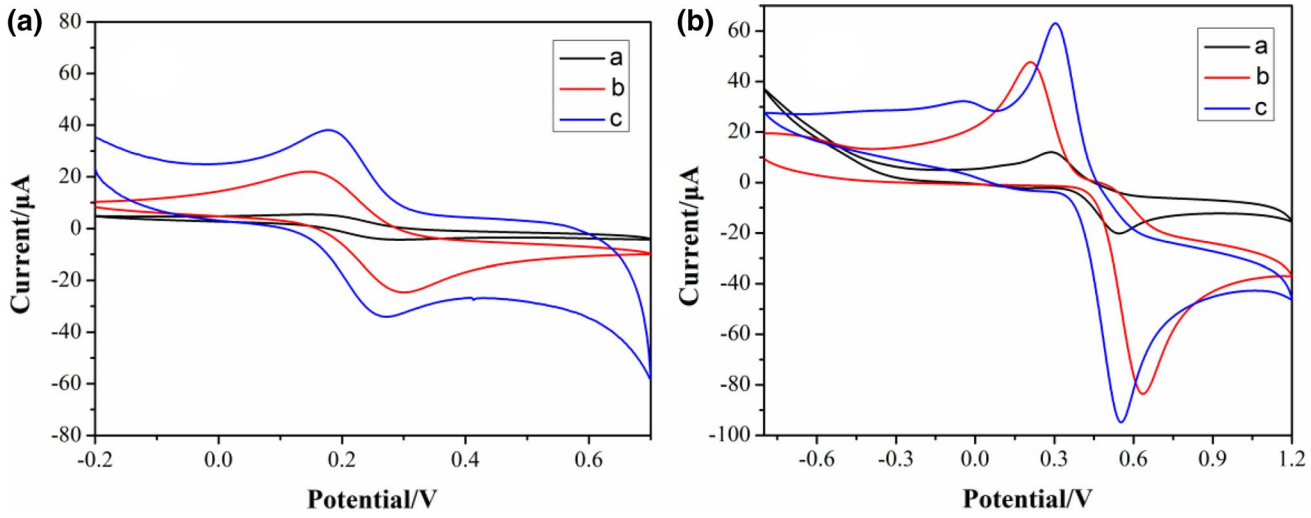

Fig. 4 **A** CVs of (a) Bare GCE, (b) Cl–GO/GCE, (c) FePP–Cl–GO/GCE in the 0.1 mol/L PBS (pH 7.0) containing 5.0 mmol/L $[Fe(CN)_6]^{3-/4-}$ and 0.1 mol/L KCl. **B** CVs of (a) Bare GCE, (b) Cl–GO/GCE, (c) FePP–Cl–GO/GCE in the 0.1 mol/L PBS (pH 7.0) containing 0.1 mol/L catechol

(002) [21]. Other miscellaneous peaks are attributed to the introduction of FePP and consistent with our previous work [22]. It was indicated that graphene oxide could be used as a covalent carrier of FePP. At the same time, the conductivity of FePP–Cl–Go would not be reduced due to excessive oxidation of graphene.

Electrochemical behavior of the proposed biosensor

Figure 4A presented the CV scanning results of bare GCE, Cl–GO/GCE and FePP–Cl–GO/GCE electrodes. Redox peaks in the potential range of − 0.8 to 0.2 V were observed on all the electrodes. Compared with the bare electrode, the current values of Cl–GO/GCE and FePP–Cl–GO/GCE electrodes were increased by 17 and 33 μA, respectively. These behaviors reflected that Cl–GO greatly enhanced the electrochemical performance of FePP. The excellent conductivity and large specific surface area of Cl–GO offered abundant active sites for the loading of FePP [23]. Under the action of a small molecule coupling agent ionic liquid, both the electron transfer during FePP catalytic oxidation [24] and the bond between FePP and Cl–GO were promoted to make the biosensor more stable. Figure 4B presented the cyclic voltammetry of various electrodes in 0.1 M catechol solution (pH 7.0). As shown in curve a, a weak redox peak of the bare electrode was obtained due to the self-oxidation of catechol. In contrast, as shown in curve b, an obvious redox peak of Cl–GO-modified electrode appeared, and the amplification of the electrical signal was due to the self-oxidation of catechol. It proved the excellent electrical conductivity of the modified material. As shown in curve c, a higher redox peak of FePP–Cl–GO-modified electrode appeared indicating that FePP promoted phthalate catalytic oxidation of catechol.

EIS was used to study the interface characteristics of the electrode surface charge transfer process, including high frequency semicircular and low frequency linear (Fig. 5). The semicircular diameter represented the electron transfer resistance (Ret), which dominated the electron transfer kinetics of the electrode interface redox probe. The linear portion was attributed to the diffusion limit process [25]. The impedance spectra in Fig. 5 revealed that the bare GCE exhibited a large semicircle with a Ret value of 2000 Ω. As shown in Fig. 5, it was hard to obtain Ret value of the synthesized nanomaterials, which was attributed to ultra-low impedance of grapheme oxide. Apparent decrease of Ret after GO was immobilized on the surface of GCE indicated that electron transfer on the surface of the electrode became easier. The slightly increased Ret of FePP–Cl–GO/GCE was probably because of the existence of FePP that hindered electron transfer on the electrode surface [26].

The influence of scan rate on the CV response of the FePP–Cl–GO/GCE in PBS solution (pH 7) with 0.1 mol/L KCl and 0.1 mol/L catechol was shown in Fig. 6a. At a relatively slow scan rate, the oxidation–reduction process of the nanocomposite presented basically symmetric anode and cathode peaks. When the scan rate increased, the redox potential of catechol slightly changed. The anode and cathode peak currents (Ipa, Ipc) increased linearly with the scan rate

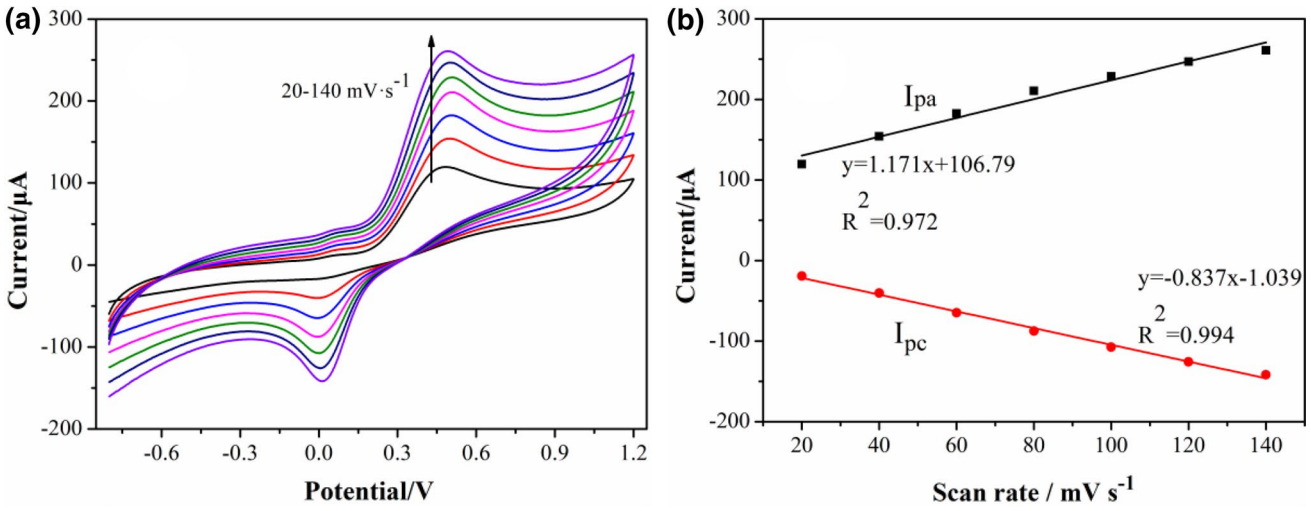

Fig. 6 **a** CV of FePP–Cl–GO/GCE in PBS solution (pH 7) with 0.1 mol/L KCl and 0.1 mol/L catechol at different scan rates of 20, 40, 60, 80, 100, 120, 140 mV/s. **b** The plots of anodic and cathodic peak current vs. scan rate

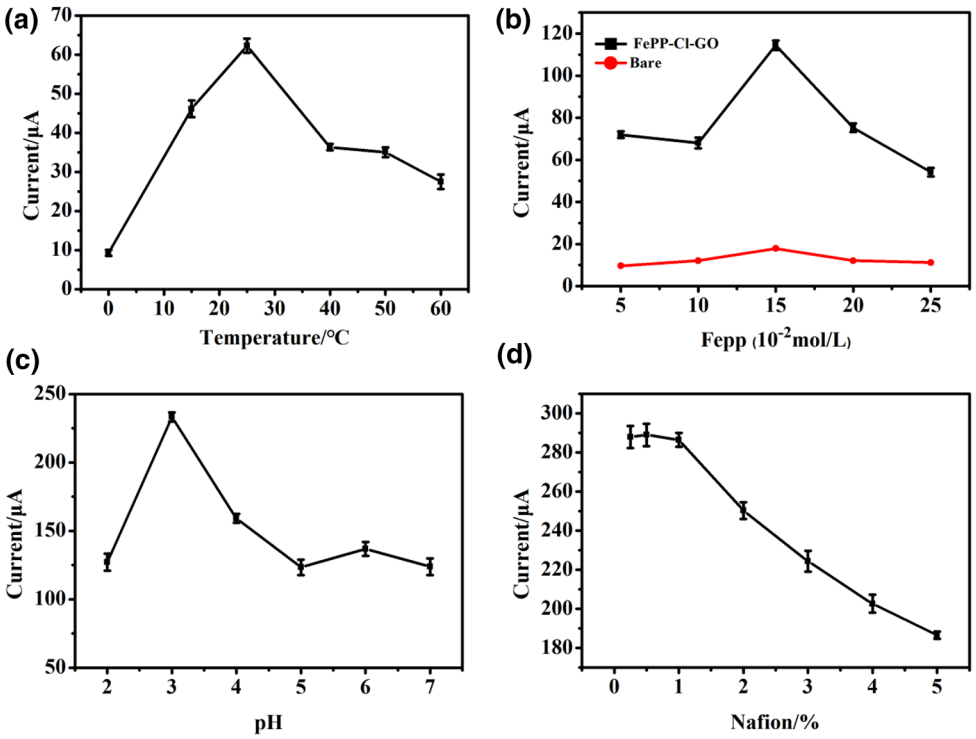

Fig. 7 **a** FePP–Cl–GO/GCE in 0.1 M PBS (pH 7.0) containing 0.1 mol/L catechol with different temperature values. **b** FePP–Cl–GO/GCE in 0.1 M PBS (pH 7.0) containing 0.1 mol/L catechol with different FePP loading values at optimal temperature **c** FePP–Cl–GO/GCE in 0.1 M PBS with different pH values containing 0.1 mol/L catechol at optimal temperature and FePP loading. **d** FePP–Cl–GO/GCE in 0.1 M PBS (pH 3.0) containing 0.1 mol/L catechol with different Nafion volume at above optimal conditions. Scan rate: 100 mV/s

from 20 to 140 mv/s. It showed that the redox reaction of catechol on FePP–Cl–GO-modified electrode was a quasi-reversible surface control process. The cathode peak current had a linear relationship with the scan rate curve (Fig. 6b). The linear regression equation was: Ipa (μA) = 1.171X + 106.79, Ipc (μA) = − 0.837X− 1.039, and the correlation coefficients (R^2) were 0.972 and 0.994, respectively. These results proved the fast DET kinetics of catechol on the FePP–Cl–GO-modified electrode surface.

Optimization of parameters

Figure 7 demonstrated the effect of the reaction temperature on the FePP–Cl–GO/Nafion/GCE electrodes in the range of 0–60 °C in a 0.1 mol/L catechol buffer solution. The results were detected by CV scanning. The peak current difference between the biomimetic oxidase and bare electrode shown in Fig. 7a confirmed the oxidation of catechol catalyzed by biomimetic enzyme sensor. It was seen that catechol did not self-oxidize lower than 25 °C. A gradual catalytic activity increase was observed at higher temperature. When the temperature was higher than 40 °C, the sharply decreased current verified the instability of catechol [27]. Therefore, 25 °C was chosen as the best measurement temperature.

In this study, FePP was substituted for horseradish peroxidase to rapidly detect the content of catechol, so optimizing

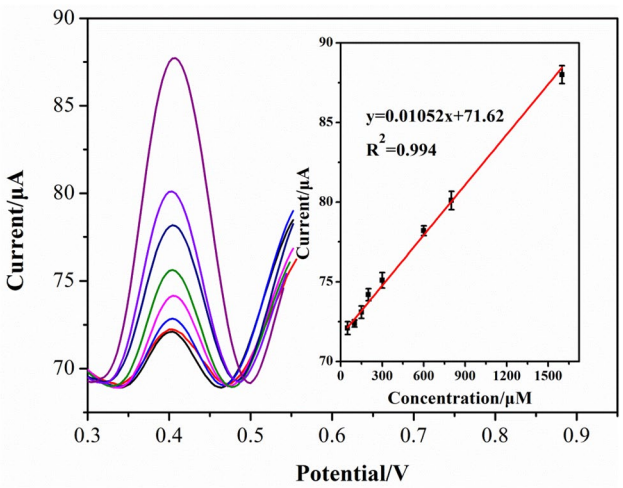

Fig. 8 DPV curves peak current of FePP–Cl–GO/Nafion/GCE electrode in air-saturated solution with the concentrations of catechol varying from 5.0 to 1600.0 μmol L^{-1} (Left). Standard curve of the catechol solution concentration was measured in 0.1 mol/L PBS buffer (pH 3.0) at 25 °C (right)

the amount of FePP was necessary. As shown in Fig. 7b, the oxidation of catechol was promoted with the increased amount of FePP because catechol was supersaturated and the FePP involved was insufficient to catalyze all the substrate.

Table 1 Different sensor results for catechol detection

Electrode	Sensitivity μA/mM	Linear range (μM)	LOD (μM)	References
AuNPs/ZnO/Al_2O_3/GO/chit/GCE	–	0.5–40	3.1	[30]
NCNTFs/GCE	–	40–120	0.12	[31]
Lac/Au-CTAB/GO/GCE	37.16	0.1–5 16.7–166	1.5	[32]
Lac/MWCNT-COOH/AuNPs-SDBS/PEDOT/GCE	12.4	11.99–94.11	12.26	[33]
PNR/MCPE	–	10–100	6.46	[34]
FePP/MWCNT/Nafion/GCE	–	65–1600	3.75	[35]
FePP–Cl–GO/Nafion/GCE	10.72	5–1600	0.09	This work

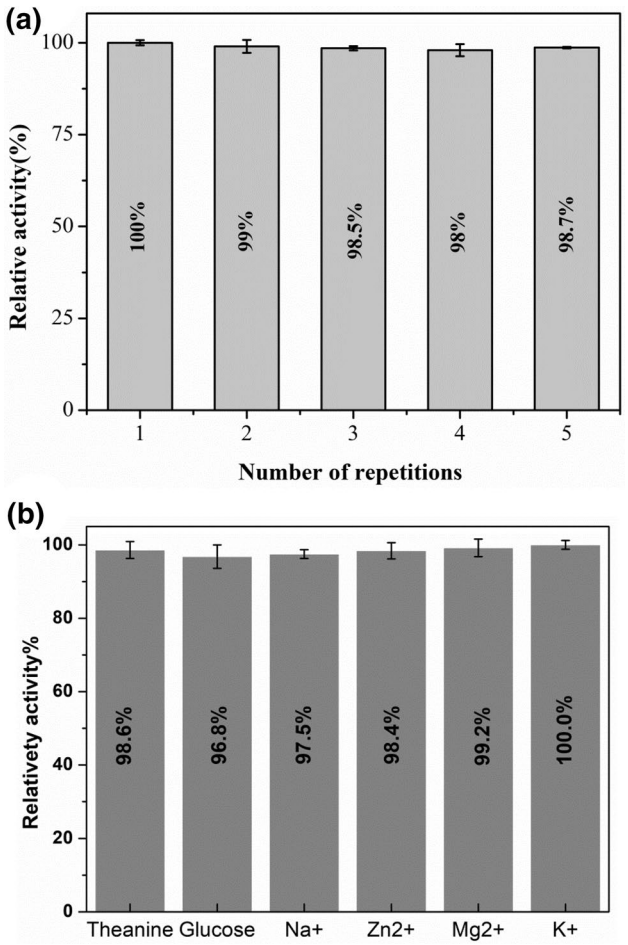

Fig. 9 Repeatability of FePP–Cl–GO/Nafion/GCE compared with the initial peak current in the 0.1 mol/L PBS buffer (pH 3.0) containing 0.1 mol/L catechol

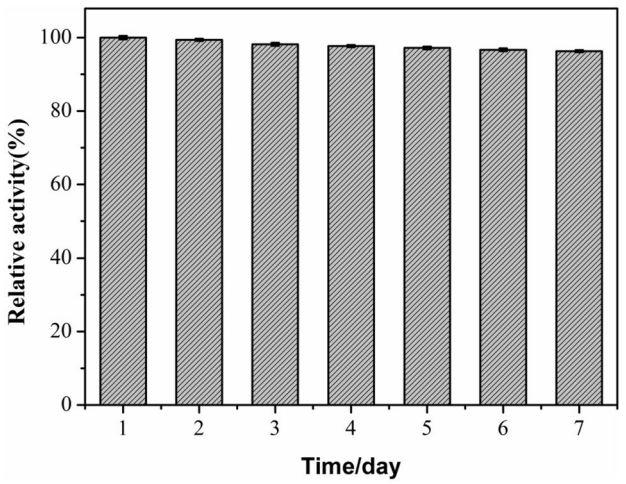

Fig. 10 Relative activity of FePP–Cl–GO/Nafion/GCE compared with the initial peak current in the 0.1 mol/L PBS buffer (pH 3.0) containing 0.1 mol/L catechol at 4 °C storage

However, the catalytic activity per unit FePP was maximal when the concentration of FePP was 1.5×10^{-3} mol/L and the value gradually declined afterward due to the limited effective surface area and electron transfer resistance. Initially, the catalyst was dispersed on surface of the electrode. As the concentration of FePP increased, the catalysts packed and thickened, which aggravated the electron transfer resistance [28]. Therefore, 1.5×10^{-3} mol/L FePP was chosen as the optimum amount of catalyst.

Effects of pH on the electrochemical reaction of FePP–Cl–GO/Nafion/GCE electrode were measured in the pH range of 2.0–7.0 in 0.1 mol/L catechol buffer solutions, the CV scanning results were shown in Fig. 7c. The optimum pH of FePP–Cl–GO/Nafion/GCE electrode was 3.0. Due to the continuous increment of the pH value, the peak current declined rapidly. It was deduced that the structure of catechol was maintained since the reaction system in the acidic environment was unfavorable to the ionization of H^+ of catechol. Under neutral or alkaline conditions, the catechol structure was destroyed and unable to participate in the oxidation catalytic reaction [29]. Therefore, pH 3.0 was chosen as the optimum pH of the reaction system.

Nafion had the potential to greatly improve the stability of the biosensor once its concentration was high enough

Table 2 Recovery experiment of detection of catechol in real water and tea samples

Samples	Number	C_{added} ($\times 10^{-5}$ mol/L)	C_{found} ($\times 10^{-5}$ mol/L)	Recovery (%)	RSD (%, $n=3$)
Water	1	30	30.16	100.53	3.9
	2	50	52.90	105.79	3.5
	3	100	95.55	95.55	4.0
Tea	1	–	6.28	–	3.2
	2	10	17.38	106.76	3.7
	3	20	25.35	96.46	3.6

[a]The content of catechol in tea was 60.2 μmol/L calculated by HPLC analysis results

because of its good adhesion and proton conductivity. However, too much Nafion limited the conduction of electrons due to its poor electrons transfer ability. It can be seen from Fig. 7d that the current change was minor when the volume ratio of Nafion was less than 1%. As the concentration increased, the current value gradually decreased. Therefore, 1% (v/v) Nafion was added to enhance the stability of the biosensor.

Detection of catechol by FePP–Cl–GO/Nafion/GCE biosensor

After optimization, the standard curve of the catechol solution was measured in 0.1 mol/L buffer solution (pH 3.0) at 25 °C via the FePP–Cl–GO/Nafion/GCE biomimetic enzyme sensor prepared with 1.5×10^{-3} mol/L FePP and 1% (v/v) Nafion. As shown in Fig. 8, the oxidation peak was linearly corresponded to the substrate concentration in the range of 50.0–1600.0 μmol/L. The linear equation was I (μA) = 0.01052C + 71.62 μmol/L ($R^2=0.994$). The detection limit (LOD) calculated according to the formula LOD = 3 × SD/slope (SD was standard deviation; slope was obtained from the standard curve) was 0.09 μmol/L. The obtained results from this work and other researches are presented in Table 1. The proposed biosensor has a low detection limit (nanomolar range), and it can be used for very sensitive samples with low concentrations of catechol. As shown in Table 1, it has the better sensitivity in comparison with other biosensors [30–35]. The satisfactory results confirmed the potential of exploration biomimetic biosensor to substitute for the horseradish peroxidase sensor [36]. FePP had the advantages of easy synthesis, low cost and convenient storage.

Selectivity and stability analysis of the proposed biosensor for catechol

After five consecutive measurements in 0.1 mol/L catechol buffer solution (pH 3.0), the relative standard deviation (RSD) of the oxidation current was kept within 2.0%, indicating FePP–Cl–GO/Nafion/GCE sensors have good repeatability (Fig. 9a). Adhesive Nafion immobilized the modification material onto the electrode and made it hard to fall off, thereby improving the repeatability of the sensor. Under the optimal conditions, the same concentration (0.1 mol/L) of theanine, glucose, and inorganic salts (NaCl, $(CH_3COO)_2$ Zn, $MgSO_4$, KBr) was add into the detection solution of 0.1 mol/L catechol. The anti-interference ability of FePP–Cl–GO/Nafion/GCE was investigated. Figure 9b showed that the above possible interfering substances in tea sample did not significantly affect the selectivity of the sensor. It was attributed to the strong anti-interference ability of FePP. FePP was similar to laccase and only catalyzed the oxidation of catechol. These results could prove that FePP–Cl–GO/Nafion/GCE has excellent selectivity to catechol. Six modified electrodes were prepared under the same conditions and subjected to the detection of catechol. The RSD of 2.5% indicated that the repeatability of biomimetic enzyme sensor was better than that of horseradish peroxidase sensor [37].

The storage stability of FePP–Cl–GO/Nafion/GCE electrode was studied at 4 °C. As shown in Fig. 10, the oxidation current value still maintained 96.3% of its initial value after stored 1 week. This behavior demonstrated that the biomimetic biosensor was more stable than the horseradish peroxidase sensor [38]. It was probably because FePP was not easily inactivated compared with horseradish peroxidase.

In practical applications, the water and tea samples were diluted with pH 3.0 buffer. The concentration of catechol was measured by standard addition. As shown in Table 2, all the recoveries were above 95.0%. It confirmed the feasibility of detection of catechol in real environment via FePP–Cl–GO/Nafion/GCE electrode.

Conclusion

In this study, an original conjunction of FePP as a biomimetic oxidase, graphene oxide as a sensing material, and ionic liquids as covalent coupling agents was designed and conducted as a biosensor. The obtained biomimetic oxidase sensor FePP–Cl–GO/Nafion/GCE was constructed for the

rapid detection of catechol. The optimal detection conditions for the biosensor prepared with 1.5×10^{-3} mol/L FePP and 1% (v/v) Nafion was pH 3.0 at 25 °C. The detection limit was 0.09 μmol/L in the range of 50.0–1600.0 μmol/L. In spite of all, the repeatability, reproducibility and stability of FePP–Cl–GO/Nafion/GCE biosensors were satisfactory. After five consecutive measurements, the RSD of the oxidation current was kept within 2.0%. The RSD of the oxidation current of six FePP–Cl–GO/Nafion/GCE electrodes prepared under the same conditions was 2.5%. After stored at 4 °C for 1 week, the oxidation current value still maintained 96.3% of its initial value.

Acknowledgements The work was funded by the National Natural Science Foundation of China (No. 21406093), the Natural Science Foundation of Jiangsu province (BK20140529), the Open Project Program of State Key Laboratory of Food Science and Technology of Jiangnan University (SKLF-KF-201919), Key University Science Research Project of Jiangsu Province (14KJB530001), China Postdoctoral Science Foundation (2014M550271), and Priority Academic Program Development of Jiangsu Higher Education Institutions.

Conflict of interest The authors declare that they have no known competing financial interests or personal relationships that could have appeared to influence the work reported in this paper.

References

1. Ishii T, Minoda K, Bae M-J, Mori T, Uekusa Y, Ichikawa T (2010) Binding affinity of tea catechins for HSA: characterization by high-performance affinity chromatography with immobilized albumin column. Mol Nutr Food Res 54:816–822
2. Nsanzamahoro S, Mutuyimana FP, Han Y, Ma S, Na M, Liu J (2019) Highly selective and sensitive detection of catechol by one step synthesized highly fluorescent and water-soluble silicon nanoparticles. Sensor Actuator B Chem 281:849–856
3. Sun X, Gong Z, Cao Y, Wang X (2013) Acetylcholinesterase biosensor based on poly (diallyldimethylammonium chloride)-multiwalled carbon nanotubes-graphene hybrid film. Nano-Micro Lett 5(1):47–56
4. Sun X, Wang X (2010) Acetylcholinesterase biosensor based on prussian blue-modified electrode for detecting organophosphorous pesticides. Biosens Bioelectron 25(12):2611–2614
5. Zhai C, Sun X, Zhao W, Gong Z, Wang X (2013) Acetylcholinesterase biosensor based on chitosan/prussian blue/multiwall carbon nanotubes/hollow gold nanospheres nanocomposite film by one-stepelectrodeposition. Biosens Bioelectron 42:124–130
6. Yu S, Rao D, Sheng Q, Zheng J (2017) Simultaneous voltammetric determination of hydroquinone and catechol by using a glassy carbon electrode modified with carboxy-functionalized carbon nanotubes in a chitosan matrix and decorated with gold nanoparticles. Microchim Acta 184:3591–3601
7. Zou B, Chu Y, Xia J (2019) Biomimetic oxidase sensor based on functionalized surface of carbon nanotubes and iron prophyrins for catechol detection. Bioproc Biosyst Eng 42:279–290
8. Taniselass S, Arshad MKM, Gopinath SCB (2019) Graphene-based electrochemical biosensors for monitoring noncommunicable disease biomarkers. Biosens Bioelectron 130:276–292
9. Zhang H, Zhang H, Aldalbahi A, Zuo X, Fan C, Mi X (2017) Fluorescent biosensors enabled by graphene and graphene oxide. Biosens Bioelectron 89:96–106
10. Qi Y, Cao Y, Meng X, Cao J, Li X, Hao Q (2019) Facile synthesis of 3D sulfur/nitrogen co-doped graphene derived from graphene oxide hydrogel and the simultaneous determination of hydroquinone and catechol. Sensor Actuator B Chem 279:170–176
11. Erogul S, Bas SZ, Ozmen M, Yildiz S (2015) A new electrochemical sensor based on Fe3O4 functionalized graphene oxide-gold nanoparticle composite film for simultaneous determination of catechol and hydroquinone. Electrochim Acta 186:302–313
12. Bhanage BM, Gaikwad V, Saptal VB, Harada K, Sasaki T, Nishio-Hamane D (2018) Ionic liquid immobilized on graphene oxide containing palladium metal ion as an efficient catalyst for the alkoxy, amino and phenoxy carbonylation reactions. Chemnanomat 4:575–582
13. Rothemund P, Menotti AR (2002) Porphyrin studies. vol 1 the metal complex salts of α, β, γ, δ-tetraphenylporphine. J Am Chem Soc 70:42–63
14. Zhang W, Zong L, Liu S, Pei S, Zhang Y, Ding X (2019) An electrochemical sensor based on electro-polymerization of caffeic acid and Zn/Ni-ZIF-8-800 on glassy carbon electrode for the sensitive detection of acetaminophen. Biosens Bioelectron 131:200–206
15. Pillai KC, Chung SJ, Moon I-S (2008) Studies on electrochemical recovery of silver from simulated waste water from Ag(II)/Ag(I) based mediated electrochemical oxidation process. Chemosphere 73:1505–1511
16. Wang Y, Yang J, Sun S, Wang L, Guo T, Zhang D (2019) PtNi nanoparticles supported on electrochemically reduced porous graphene oxide for methanol oxidation reaction. Chem Phys Lett 730:575–581
17. Khalili Dermani A, Kowsari E, Ramezanzadeh B, Amini R (2019) Utilizing imidazole based ionic liquid as an environmentally friendly process for enhancement of the epoxy coating/graphene oxide composite corrosion resistance. J Ind Eng Chem 79:353–363
18. Mejias Carpio IE, Mangadlao JD, Nguyen HN, Advincula RC, Rodrigues DF (2014) Graphene oxide functionalized with ethylenediamine triacetic acid for heavy metal adsorption and antimicrobial applications. Carbon 77:289–301
19. Lan D-H, Chen L, Au C-T, Yin S-F (2015) One-pot synthesized multi-functional graphene oxide as a water-tolerant and efficient metal-free heterogeneous catalyst for cycloaddition reaction. Carbon 93:22–31
20. Castro KADF, Figueira F, Mendes RF, Almeida Paz FA, Neves MDGPMS, Cavaleiro JAS (2019) Porphyrinic coordination polymer-type materials as heterogeneous catalysts in catechol oxidation. Polyhedron 158:478–484
21. Surekha G, Krishnaiah K, Ravi N, Suvarna R (2020) FTIR, Raman and XRD analysis of graphene oxide films prepared by modified Hummers method. J Phys Conf Ser 1945:19–21
22. Zou B, Wang P, Liu Z, Xia J, Chen B, Tan Z (2019) Biomimetic oxidase based on functionalized mesoporous SiO_2 and metalloporphyrin for 5-hydroxymethylfurfural conversion. Process Biochem 86:65–72
23. Gan T, Wang Z, Shi Z, Zheng D, Sun J, Liu Y (2018) Graphene oxide reinforced core-shell structured Ag@Cu_2O with tunable hierarchical morphologies and their morphology-dependent electrocatalytic properties for bio-sensing applications. Biosens Bioelectron 112:23–30
24. Brogan APS, Hallett JP (2016) Solubilizing and stabilizing proteins in anhydrous ionic liquids through formation of protein-polymer surfactant nanoconstructs. J Am Chem Soc 138:4494–4501
25. Casero E, Parra-Alfambra AM, Petit-Domínguez MD, Pariente F, Lorenzo E, Alonso C (2012) Differentiation between graphene oxide and reduced graphene by electrochemical impedance spectroscopy. Electrochem Commun 20:63–66
26. Li S, Zhang Q, Lu Y, Ji D, Zhang D, Wu J (2017) One step electrochemical deposition and reduction of graphene oxide on screen printed electrodes for impedance detection of glucose. Sensor Actuator B Chem 244:290–298

27. Numviyimana C, Chmiel T, Kot-Wasik A, Namieśnik J (2019) Study of pH and temperature effect on lipophilicity of catechol-containing antioxidants by reversed phase liquid chromatography. Microchem J 145:380–387
28. Guo W, Pi F, Zhang H, Sun J, Zhang Y, Sun X (2017) A novel molecularly imprinted electrochemical sensor modified with carbon dots, chitosan, gold nanoparticles for the determination of patulin. Biosens Bioelectron 98:299–304
29. Madhu R, Palanisamy S, Chen S-M, Piraman S (2014) A low temperature synthesis of activated carbon from the bio waste for simultaneous electrochemical determination of hydroquinone and catechol. J Electroanal Chem 727:84–90
30. Nazari M, Kashanian S, Moradipour P, Maleki N (2018) A novel fabrication of sensor using ZnO-Al_2O_3 ceramic nanofifibers to simultaneously detect catechol and hydroquinone. J Electroanal Chem 812:122–131
31. Zheng X, Hu Y, Li H, Han B, Lin R, Huang B (2020) N-doped carbon nanotube frameworks modified electrode for the selective sensing of hydroquinone and catechol. J Electroanal Chem 861:113968–113976
32. Nazari M, Kashanian S, Maleki N, Shahabadi N (2019) Laccase immobilized onto graphene oxide nanosheets and electrodeposited gold-cetyltrimethylammonium bromide complex to fabricate a novel catechol biosensor. Bull Mater Sci 42:42–51
33. Abdul Rasol Albayati S, Kashanian S, Nazari M, Rezaei S (2019) Novel fabrication of a laccase biosensor to detect phenolic compounds using a carboxylated multiwalled carbon nanotube on the electropolymerized support. Bull Mater Sci 42:187–192
34. Sunil Kumar Naik T, Kumara Swamy B (2017) Modification of carbon paste electrode by electrochemical polymerization of neutral red and its catalytic capability towards the simultaneous determination of catechol and hydroquinone: a voltammetric study. J Electroanal Chem 804:78–86
35. Bin Z, Yanhong C, Jiaojiao X (2019) Biomimetic oxidase sensor based on functionalized surface of carbon nanotubes and iron prophyrins for catechol detection. Bioprocess Biosyst Eng 42(2):279–290
36. Bagheri N, Khataee A, Habibi B, Hassanzadeh J (2018) Mimetic Ag nanoparticle/Zn-based MOF nanocomposite (AgNPs@ZnMOF) capped with molecularly imprinted polymer for the selective detection of patulin. Talanta 179:710–718
37. Ye Y, Yan W, Liu Y, He S, Cao X, Xu X (2019) Electrochemical detection of Salmonella using an invA genosensor on polypyrrole-reduced graphene oxide modified glassy carbon electrode and AuNPs-horseradish peroxidase-streptavidin as nanotag. Anal Chim Acta 1074:80–88
38. Feizabadi M, Soleymanpour A, Faridnouri H, Ajloo D (2019) Improving stability of biosensor based on covalent immobilization of horseradish peroxidase by γ-aminobutyric acid and application in detection of H_2O_2. Int J Biol Macromol 136:597–606